

JGR Biogeosciences

RESEARCH ARTICLE

10.1029/2021JG006681

Key Points:

- Extreme weather events significantly influence the Hg biogeochemical processes in subtropical forests
- The sustained droughts increase litterfall Hg concentration and deposition, and the snowstorm promotes soil Hg burden sharply
- The accelerated climate change distinctly increases the unpredictability in assessing the effectiveness of Minamata Convention

Supporting Information:

Supporting Information may be found in the online version of this article.

Correspondence to:

X. Wang,
wangxun@mail.gyig.ac.cn

Citation:

Yuan, W., Wang, X., Lin, C.-J., Zhang, H., Feng, X., & Lu, Z. (2022). Impacts of extreme weather on mercury uptake and storage in subtropical forest ecosystems. *Journal of Geophysical Research: Biogeosciences*, 127, e2021JG006681. <https://doi.org/10.1029/2021JG006681>

Received 20 OCT 2021

Accepted 19 DEC 2021

Author Contributions:

Conceptualization: Wei Yuan, Xun Wang, Xinbin Feng

Formal analysis: Xun Wang



Funding acquisition: Xun Wang, Che-Jen Lin, Xinbin Feng

Methodology: Wei Yuan, Xun Wang, Hui Zhang, Zhiyun Lu

Writing – original draft: Wei Yuan, Xun Wang

Writing – review & editing: Che-Jen Lin, Xinbin Feng

Impacts of Extreme Weather on Mercury Uptake and Storage in Subtropical Forest Ecosystems

Wei Yuan¹, Xun Wang^{1,2} , Che-Jen Lin^{3,4}, Hui Zhang¹, Xinbin Feng¹ , and Zhiyun Lu⁵

¹State Key Laboratory of Environmental Geochemistry, Institute of Geochemistry, Chinese Academy of Sciences, Guiyang, China, ²College of Resources and Environment, Southwest University, Chongqing, China, ³Center for Advances in Water and Air Quality, Lamar University, Beaumont, MI, USA, ⁴Department of Civil and Environmental Engineering, Lamar University, Beaumont, MI, USA, ⁵Ailaoshan Station for Subtropical Forest Ecosystem Studies, Chinese Academy of Sciences, Jingdong, China

Abstract As climate change accelerates, extreme weather events become more severe and frequent. We analyzed the datasets of decade-long observation (2005–2020) of mercury (Hg) stored in two subtropical evergreen forests to understand the impacts of extreme weather on the sequestration of atmospheric Hg in forest ecosystems. Results show a weak correlation between litterfall Hg and atmospheric Hg⁰ concentration. Droughts and snowstorms significantly disturb Hg accumulation in litterfall and soils. Litterfall Hg concentration and deposition both display an increasing trend during the period of extended droughts in 2011–2014, but a decreasing trend after droughts. This is caused by the water stress that influences the change of tree physiology and processes of foliage Hg⁰ uptake. Snowstorm damages large areas of canopy, which leads to substantial canopy epiphyte cover mixed into the forest floor, thus considerably increasing soil Hg concentrations. Over a decadal timescale, soil Hg variabilities are shaped by the combined effects of atmospheric Hg inputs and processes of organic soil mineralization mediated climatic factors. Our study highlights that the accelerated climate change increases the unpredictability of Hg accumulation in terrestrial ecosystems. Future studies are needed for better understanding the response of Hg biogeochemical cycling to climate change among different terrestrial biomes.

Plain Language Summary The decade-long observation of litterfall Hg deposition and uppermost soil Hg concentration was carried out at a subtropical forest in Southwest China. Our data clearly display how the extended droughts and largest snowstorm of the past four decades at studied site influencing the foliage and soil Hg cycling. We suggest the drought would increase the litterfall Hg concentration and total deposition flux, and the snowstorm would remarkably increase the atmospheric Hg burden which derived from the canopy long-term stored Hg. We highlight that the extreme weather events could disturb the ecological balance and Hg biogeochemical Hg cycling in forest ecosystem.

1. Introduction

To protect human health and the environment from impacts of anthropogenic mercury (Hg) emissions, Minamata Convention on Mercury, a legally binding international treaty, entered into force in August 2017. However, significant knowledge gaps in Hg cycling challenge our ability to assess the effectiveness of the Convention in reducing human and wildlife Hg exposure (Outridge et al., 2018; Selin et al., 2018; UN-Environment, 2019). Currently, the annual anthropogenic Hg emissions into the atmosphere are estimated to be 1900–2200 Mg, only accounting for ~30% of total Hg emissions, whereas up to 60% of the total Hg emissions are contributed from re-emissions of previously deposited Hg (legacy Hg) (Outridge et al., 2018; UN-Environment, 2019). Several field observations and model simulations predict that land-use and climate change can profoundly alter the Hg biogeochemical cycling, as they directly affect the legacy Hg re-emissions from the terrestrial and ocean pools (S. Sun et al., 2020; Wang, Luo, et al., 2020; Y. Zhang et al., 2020). While a reduction of anthropogenic Hg emissions is expected to distinctly decrease the Hg concentration in the atmosphere, as have been observed at Northern Hemisphere Remote sites (Tang et al., 2018; Zhang, Jacob, et al., 2016), it may take much longer for biotic Hg, especially Hg in aquatic biota, to decrease due to complex processes associated with climate change and changes in land-use and ecosystems (Braune et al., 2016; Burgess et al., 2013; Evans et al., 2013; Wang, Outridge, et al., 2019).

Terrestrial biota is less prone to Hg bioaccumulation since the conversion of inorganic Hg to methyl Hg is generally not favored in the terrestrial environment (Bushey et al., 2008; Douglas et al., 2012). However, terrestrial soil represents the largest global Hg pool, with an estimated 1100 Gg Hg being stored in top 0–20 cm surface soils (Wang, Yuan, Lin, et al., 2019). It is an important sink of atmospheric Hg with a deposition flux of 3200–3600 Mg yr⁻¹ (Outridge et al., 2018). As such, climate change can significantly reshape Hg accumulation in soils (Wang, Luo, et al., 2020), re-emissions back to atmosphere (Gabriel et al., 2005), and transport to downstream aquatic ecosystems where methyl Hg is produced, bioaccumulated and biomagnified (Evers et al., 2007; Feng et al., 2010). Therefore, the storage and translocation of Hg in terrestrial ecosystems and its response to climate change are important in the assessment of global Hg mass budget and have implication on the effectiveness of the Minamata convention. As climate change accelerates, extreme weather events become more severe and frequent, which affect the ecological resilience of terrestrial ecosystems (Gastineau & Soden, 2009; Orłowsky & Seneviratne, 2012). Studies on terrestrial ecosystems in temperate and boreal regions have revealed that extreme storms (Allan et al., 2001; Bushey et al., 2008; Eklof et al., 2013; Lee et al., 2000) and pulses of snowmelt and melting glaciers (Douglas et al., 2017; X. J. Sun et al., 2017) could result in elevated Hg runoff into downward aquatic ecosystems. However, much less data are available for subtropical and tropical forest ecosystems where 60%–70% of global litterfall Hg deposition and surface Hg storage reside (Wang, Bao, et al., 2016; Wang, Yuan, Lin, et al., 2019).

In this study, we hypothesized that the extreme weather events have considerable effects on Hg uptake and accumulation in subtropical forests. Decade-long datasets of meteorological factors and Hg distributions in atmosphere, litterfall and soils in two subtropical evergreen forests are analyzed for examining how the Hg content in litter and soil samples responds to extreme weather and changes of atmospheric Hg concentrations. We finally discussed the implications of forest Hg cycling in the context of climate change.

2. Materials and Methods

2.1. Site Description

The study sites are located at 2,450–2,650 m above the sea level (asl) within the Ailaoshan Station for Subtropical Forest Ecosystem Research Studies (ASSFERS), southwest China. ASSFERS has China's largest subtropical montane evergreen forest ecotone because of its relatively warm and wet climate and remote location with minimal human's disturbance (Z. Y. Lu et al., 2016; Wang, Lin, Lu, et al., 2016; Wang, Yuan, Lu, et al., 2019; Yuan, Sommar, et al., 2019; Yuan, Wang, et al., 2019; W. Yuan et al., 2020). Our earlier studies have reported the atmospheric Hg deposition, Hg storage in soils, and Hg isotopic signatures at ASSFERS (Z. Y. Lu et al., 2016; Wang, Lin, Lu, et al., 2016; Wang, Yuan, Lu, et al., 2019; W. Yuan et al., 2020), and in this study we examine the response of forest Hg to extreme weather. We selected two forest types. One is the old-growth moist evergreen broadleaf (MEB) forest that is located at around 2,450 m asl (101.0263 E, 24.5391 N), with an average canopy height of 20–25 m. The dominant tree species are *Castanopsis wattii*, *Lithocarpus xylocarpus*, *Schima noronhae* and *Manglietia insignis*. The other is the summit mossy dwarf (SMD) forest that occupies at higher elevations (2,600–2,650 m asl), with a 5–7 m canopy layer and >85% canopy coverage. The dominant tree species in the SMD forest are *pachyphyllodes* L. and *Rhododendron irroratum*. The annual precipitation at ASSFERS is about 1800 mm with distinct dry (November to April) and rainy (May to October) seasons; 85% of precipitation occurs in the rainy season. The mean annual temperature is 13.0 ± 5.0°C (average ± standard deviation), and mean annual relative humidity is 84% ± 5% (Z. Y. Lu et al., 2016; Wang, Lin, Lu, et al., 2016). The forest soil at both sites is mainly Luvisol (World Reference Base) with a pH of 3.5–3.9 (Wang, Lin, Lu, et al., 2016; W. Yuan et al., 2020).

2.2. Collection and Measurements of Litterfall and Soil Samples

We collected monthly litterfall samples at the two forest sites ($n = 25$ for MEB and $n = 12$ for SMD in each month) from January 2005 to December 2019. The collection methodology has been documented in our earlier studies (Wang, Lin, Lu, et al., 2016; Wang, Yuan, Lu, et al., 2019). Briefly, monthly litterfall samples were collected by 1 × 1 m nylon nets hanging 1 m above ground at 25 random locations at MEB, and 12 random locations at SMD forests. Litterfall samples were placed in paper bags and dried at 50°C in an oven for 72 hr. Our earlier studies have shown this drying process would not lead to Hg loss from vegetation (Wang, Yuan, et al., 2020). After being dried, litterfall samples were ground in an electric grinder, sieved with a 200-mesh (74 μm) sieve,

and the fraction passed through the sieve was placed in Hg-free plastic bags for chemical analysis. Litter samples from 2005 to April, 2011 were only measured the total biomass, and samples from May, 2011 to 2019 were measured total biomass and Hg concentration. The litter Hg concentration results at ASSFERS were reported by Zhou et al. (2013), B. Yu et al. (2016), Wang, Lin, Lu, et al. (2016), Wang, Yuan, Lu, et al. (2019) and W. Yuan et al. (2020). Our litterfall Hg data are new and based on the sampling methodology of this study. It is noted that some our data are comparable to earlier reported values, because of similar sampling locations, time periods and tree species. The litterfall samples included litter of leaf, bark, twig, moss, flower, fruit, and other detritus litters. Our earlier study in 2013 (Zhou et al., 2013) and analysis of litterfall Hg deposition in 2019 (see Table S1 in Supporting Information S1) both suggest that leaf litter Hg accounts for about 70% of the total litterfall Hg deposition. Hereafter, “litterfall” refers to leaf litter only, unless otherwise specified.

For forest soil sampling, six replicates of 10 m × 10 m subplots were established at each site (Z. Y. Lu et al., 2016; Wang, Lin, Lu, et al., 2016; Wang, Yuan, Lu, et al., 2019). We mainly collected forest humus soils (3–5 cm depth from the forest floor; reflecting short-term (decadal) variations and top mineral soils (0–20 cm; reflecting long-term [hundreds of years] variations in this study. Briefly, 12 replicate samples were selected from each sampling subplot to form an “S” shape and then mixed to produce a composite sample (1–2 kg in mass). Six composite samples were collected from each forest type during one sampling event. The same approach was utilized for both the humus and top mineral soils. During 2007–2015, the soil samples were collected at the end of dry (April to May) and rainy (October to November) seasons with 24 samples for MEB and for SMD in each year. During 2016–2020, we collected 12 soil samples in each April for MEB and for SMD. The soil samples were air dried and sieved following the same approach as the vegetation samples, and the <74 μm fractions were placed in Hg-free plastic bags for chemical analysis. Our earlier study has suggested several days air drying at clear room (air Hg⁰ concentration less than 5 ng m⁻³) lead to <3% influence on soil Hg concentration (Wang, Lin, Lu, et al., 2016).

Mercury concentrations in vegetation and soil samples were measured by a DMA80 Hg analyzer. We measured Hg concentrations in leaf litterfall samples collected in May 2011–July 2014, August 2015–January 2018, and January 2019–December 2019 in MEB forest, and August 2015–January 2018 in SMD forest. Standard reference materials GBW07405 (GSS-5, soil, Hg = 290 ± 40 ng g⁻¹), GBW10020 (GSB-11, vegetation, Hg = 150 ± 25 ng g⁻¹) and GBW10049 (GSB-27, vegetation, Hg = 12 ± 3 ng g⁻¹, all from National Standard Reference Materials of China) were used for QA/QC and measured every 9 samples with a recovery of 95%–105%. In addition, we utilized the Walkley-Back method (i.e., using Cr₂O₇²⁻ to oxidize soil organic carbon, and then FeSO₄ to reduce the excess Cr₂O₇²⁻) to determine soil organic carbon (OC) content (Walkley, 1947). Litterfall and soil Hg data for two forest sites can be found in Supporting Information S1.

2.3. Litterfall Hg Deposition and Atmospheric Total Hg

The litterfall Hg deposition was estimated by:

$$J_{\text{Litter}} = C_{\text{Hg}} \times P_{\text{Litter}} \quad (1)$$

where J_{Litter} is the litterfall Hg deposition flux (unit: μg m⁻² month⁻¹), C_{Hg} is litterfall Hg concentration (unit: ng g⁻¹), and P_{Litter} is the monthly biomass production of litterfall (unit: g m⁻²). The atmospheric total gaseous Hg (TGM), >99% of which is Hg⁰ at ASSFERS (Zhang, Fu, et al., 2016) has been measured at ASSFERS by Tekran 2537 Mercury Analyzer since May of 2011, following the protocol of GMOS (Global Mercury Observation System) (D'Amore et al., 2015) as described elsewhere (Wang et al., 2015; H. Zhang, Fu, et al., 2016). Briefly, the Tekran system was automatically calibrated for Hg⁰ every 73-hr using an internal permeation source, which provides ~1 pg s⁻¹ of Hg⁰ at 50°C into the zero-air stream. External calibration using a Tekran 2505 Mercury Source with manual injections of known concentrations of Hg⁰ was performed every 4 months. For assessing the impact of TGM on Hg accumulation in litterfall, “AccuTGM” was defined to represent the mean TGM concentration during the foliage lifespan (approximately 1 year at ASSFERS (Wang, Lin, Lu, et al., 2016)):

$$\text{AccuTGM}_i = \frac{\sum_{i-13}^{i-1} \text{TGM}}{12} \quad (2)$$

where AccuTGM_i is the mean TGM concentration during foliage lifespan for the i -th month litterfall, for example, for the leaf litter sampled in June 2012, the corresponding AccuTGM was calculated as the average TGM

concentration during June 2011 to May 2012. In this study, we analyzed the relationship between AccuTGM and litterfall Hg concentration during 2012–2019.

2.4. Meteorological Data

The Meteorological data including precipitation amount, solar radiation, potential evapotranspiration, and air temperature 2 m above the ground level were Measured at a nearby station by the Chinese Academy of Sciences, following the protocols of the Chinese Ecosystem Research Network (QX/T 50–2007 and QX/T 51–2007). The Meteorological station is located at 2,450 m asl, and about 1 km away from our selected forest sites. We used the reconnaissance drought index (RDI) which is based on cumulative precipitation and potential evapotranspiration to assess the severity of drought (Tsakiris et al., 2007)

$$a_k^i = \frac{\sum_{j=1}^{j=k} P_j}{\sum_{j=1}^{j=k} PET_j} \quad (3)$$

$$RDI^i = \frac{\ln a_i - \overline{\ln a}}{\hat{\sigma}} \quad (4)$$

where a_k^i is the initial value of RDI, P_j and PET_j are the precipitation and potential evapotranspiration of the j -th month of the i -th hydrological year. The hydrological year at ASSERFES starts in November, hence for November $k = 1$. $\hat{\sigma}$ is standard deviation of $\ln(a_k^i)$. The RDI is estimated by periods of 3, 6, 9 and 12 months in each hydrological year and the drought event is defined as a period commencing when $RDI < -1$ based on earlier studies (Cheng et al., 2020; Tsakiris et al., 2007).

2.5. Statistical Methods

We used the R Programming Language to remove outliers (those that are out of the range between the upper extreme and lower extreme values in a box and whiskers plot) in each data set. The Kolmogorov-Smirnov test was applied to decide if the data of a sample not came from a normal distribution. Student's t -test and One-Way ANOVA test (if homogeneity of sample variance, otherwise using Kruskal-Wallis test) were used to infer statistical differences among groups. Linear and polynomial regressions with F -test or t -test were used to examine their relationships. These statistical analyses were performed by SPSS version 22.0 at a confidence level of 95%.

3. Results and Discussion

3.1. Impacts From Extreme Weather on Litterfall Biomass Production

Figure 1 shows monthly rainfall, RDI, and litterfall biomass production in MEB and SMD forests from January 2005 to December 2019. The distinct dry (November to April) and rainy (May to October) climate at ASSERFES (Figure 1a) leads to the seasonal litterfall biomass production with a bi-modal pattern (Liu et al., 2003), that is, one peak in the early dry season (November to December) and the other at the beginning of the rainy season (April to May), respectively (Figures 1b and 1c). The litterfall biomass peak in the earlier dry season of the MEB forest is significantly lower than that during April to May ($P = 0.000$ by independent t -test, Figure 1b). However, the two peaks are comparable in the SMD forest ($P = 0.35$ by independent t -test, Figure 1c). This is because the different tree species and the deeper soil depths in the MEB forest can sustain more foliage growth in the dry season. The annual litterfall biomass production in the MEB forest is 16% higher than that in the SMD forest, consistent with the higher net primary productivity in the MEB forest (Liu et al., 2002; Xu et al., 2020).

Notably, extended droughts occurred during November 2011–August 2014, marked by a decreasing trend of RDI with $RDI < -1$ throughout the dry seasons (Figure 1a). Drought-induced water stress promotes leaf senescence in subtropical forests (Liu et al., 2003), evidenced by an increasing litterfall biomass production during this drought period (Figures 1b and 1c). The litterfall biomass production during November 2013–May 2014 increased 50% in the MEB forest ($p < 0.01$, Independent-samples t -test) and 33% in the SMD forest ($p = 0.43$, Independent sample t -test) in comparison to the values during November 2011–May 2012. The distinct drought events in the dry seasons of 2006, 2008, and 2010 are also associated with an elevated litterfall biomass production in MEB and SMD

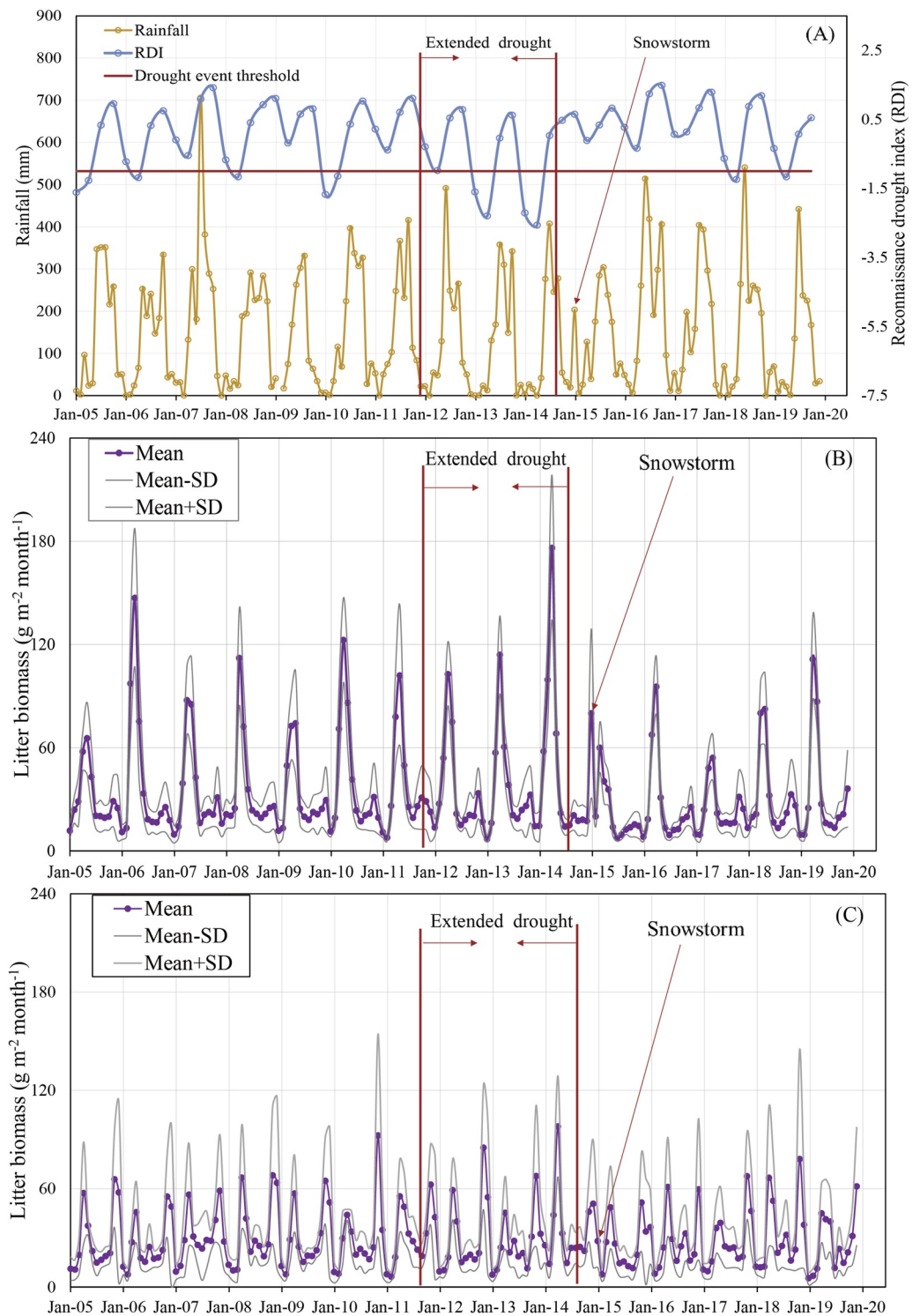


Figure 1. (a) Temporal trend of rainfall and reconnaissance drought index (RDI), (b) temporal trend of litterfall biomass production for mature evergreen broadleaf (MEB) forest, (c) temporal trend of litterfall biomass production for summit mossy dwarf (SMD) forest during January 2005 to December 2019.

forests. The largest snowstorm in the past four decades at ASSFERS happened on January 9th to 11th 2015 (Song et al., 2017). During a short span of three days, roughly 40 cm of snow fell on the plot, resulting in a large number of broken tree branches, and the average leaf area index decreased from 3.85 ± 0.51 (Mean \pm standard deviation) before the snowstorm to 2.21 ± 0.47 afterwards (Song et al., 2017). The snowstorm induced a pulse of litterfall deposition in January 2015 (Figure 1c), but the annual litterfall biomass production decreased by 29%–40% when comparing the production between the year of 2014 and 2015 (Figure S1 in Supporting Information S1).

3.2. Impacts From Extreme Weather on Litterfall Hg

The monthly litterfall Hg concentration in the MEB forest ranges from 43 ± 10 ng g⁻¹ to 80 ± 17 ng g⁻¹ during 2011–2019, with an overall average of 60 ± 13 ng g⁻¹ ($n = 650$ samples). In the SMD forest, the value ranges from 38 ± 7 ng g⁻¹ to 81 ± 7 ng g⁻¹ with an overall average of 57 ± 8 ng g⁻¹ ($n = 210$). The litterfall Hg concentrations in MEB and SMD forests show insignificant difference ($P = 0.101$ by independent t -test), but are significantly correlated ($r = 0.78$, $P = 0.000$ by t -test), indicating that they are driven by similar processes. The concentrations are in good agreement with our earlier study (Wang, Lin, Lu, et al., 2016) on 29 evergreen broadleaf (EB) forests (60 ± 30 ng g⁻¹), which are significantly higher than those reported for temperate and boreal forests (43 ± 12 ng g⁻¹, $n = 89$ sites, $P < 0.01$ by independent t -test) (Wang, Bao, et al., 2016). The difference has been attributed to the combined effects of 1–2 years leaf lifespan and stronger foliage assimilation of EB tree species (Seyoum et al., 2012; Wang, Bao, et al., 2016).

The monthly litterfall Hg deposition in the MEB forest ranges from 0.6 ± 0.2 to 11.7 ± 4.1 μg m⁻² month⁻¹, with an overall mean monthly deposition of 2.0 ± 1.8 μg m⁻² month⁻¹. In the SMD forest, it ranges from 0.5 ± 0.2 μg m⁻² month⁻¹ to 4.8 ± 3.5 μg m⁻² month⁻¹, with an overall mean monthly deposition of 1.6 ± 0.9 μg m⁻² month⁻¹ (Figures 2a and 2b). These values are 30%–40% lower than those reported in our earlier studies (Wang, Yuan, Lu, et al., 2019; W. Yuan et al., 2020), because the litterfall refers mainly to the leaf litterfall in this study, but includes all the litterfall in our earlier studies. The r value between litterfall Hg deposition and litterfall biomass production is up to 0.99, much higher than that (0.26) between litterfall Hg deposition and litterfall Hg concentration (Figure 3a). The temporal trends of litterfall Hg deposition in the MEB and SMD forests are controlled predominantly by the pattern of litterfall biomass production, consistent with earlier studies (Wang, Lin, Lu, et al., 2016; Wang, Yuan, Lu, et al., 2019). The elevated litterfall Hg deposition usually occurs in early winter and late spring when biomass production peaks. The annual litterfall Hg deposition after snowstorm (2015–2016) is 90%–120% lower than the deposition before the snowstorm (2013–2014) which attributed to the combining effect from the decrease of litterfall biomass production caused by the snowstorm and the elevated litter Hg concentration during 2013–2014 (Figure 2a).

Litterfall Hg concentrations in the MEB forest during 2011–2019, and in the SMD during 2015–2017 do not exhibit a significant temporal trend (both $r = 0.0$, $P > 0.05$ by t -test; Figures 2a and 2b). During the period of sustained drought in Nov 2011 to Aug 2014, the litterfall Hg concentration in MEB shows a significant increasing trend with time ($r = 0.65$, $P < 0.01$ by t -test), with an average rate of 0.5 ng g⁻¹ month⁻¹, and the Hg concentration peaks at the same time as litterfall biomass production (Figure 2a). Following the drought period, a significantly decreasing trend of litter Hg concentration is observed in MEB and SMD forests, respectively (Figures 2a and 2b). The litterfall Hg displays an average decreasing rate of -1.7 ng g⁻¹ month⁻¹ in the MEB forest ($r = -0.82$, $P < 0.01$ by t -test) and -1.5 ng g⁻¹ month⁻¹ in the SMD forest ($r = -0.72$, $P < 0.01$ by t -test) from August 2015 to September 2016. Given that litterfall Hg is mainly derived from atmospheric Hg⁰ (Wang, Luo, et al., 2017; Wang, Luo, et al., 2020), this change can be attributed to the variations in atmospheric Hg⁰ and in tree physiological processes.

Air–foliage Hg⁰ exchange is a dynamic bi-directional process including atmospheric Hg⁰ deposition and foliage Hg evasion (Hanson et al., 1995; X. Wang et al., 2014; Wang, Lin, Yuan, et al., 2016). An elevated atmospheric Hg⁰ concentration enhances Hg⁰ deposition flux, potentially resulting in higher Hg concentration in foliage. Measurements at ASSFERS show that the mean TGM concentration decreased from 2.1 to 1.4 ng m⁻³ from 2011 to 2014, and has stayed at the level of 1.4 to 1.6 ng m⁻³ since then (Sprovieri et al., 2016; X. Wang et al., 2015; Zhang, Fu, et al., 2016). Similarly, AccuTGM decreased from 2.1 ng m⁻³ in January 2012 to 1.4 ng m⁻³ in December 2014 and was near constant at 1.3–1.4 ng m⁻³ from August 2015 to September 2016 (Figure 2a). The litterfall Hg concentration shows no significant correlations with AccuTGM (all $r = 0.0$, $P > 0.05$ by t -test). The temporal changes in litterfall Hg cannot be explained by the variation in AccuTGM nor atmospheric Hg⁰.

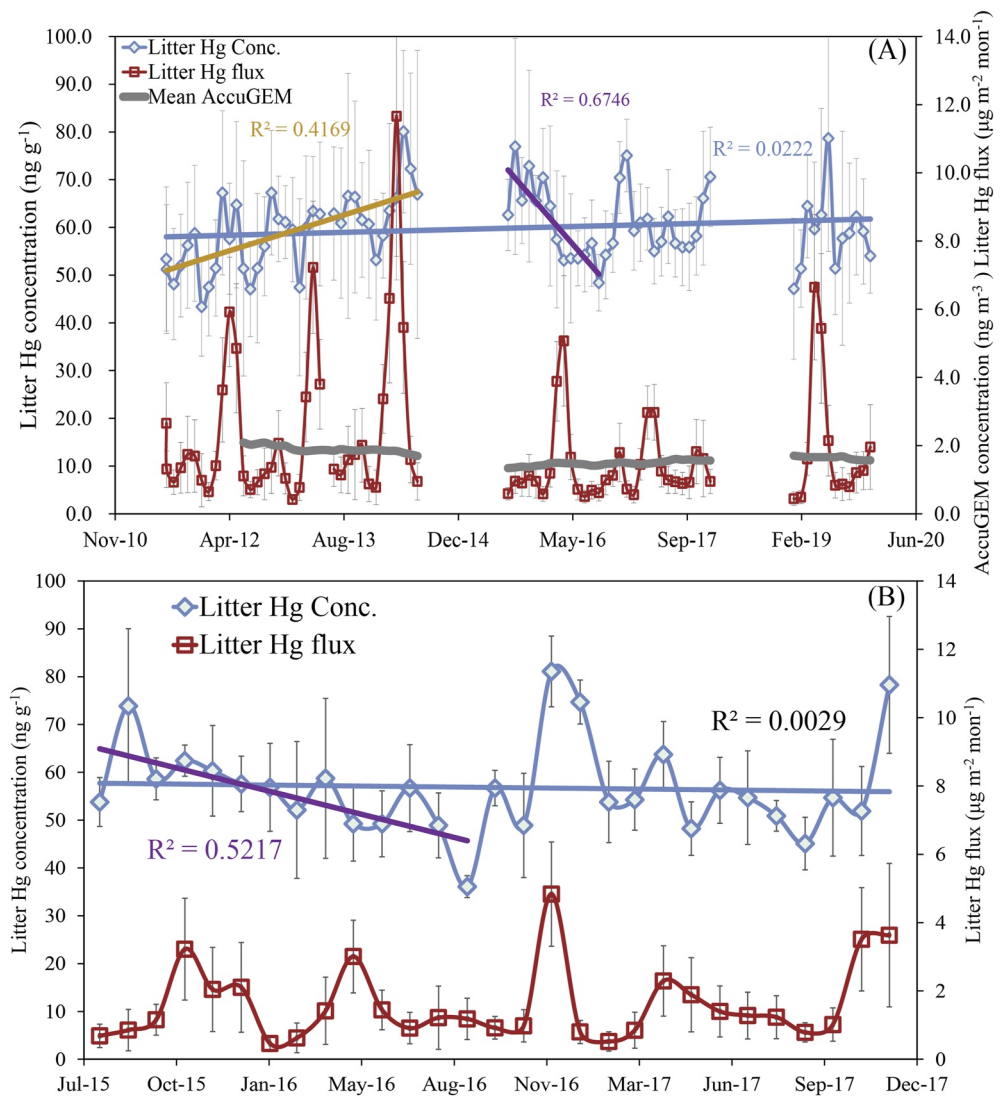


Figure 2. Monthly mean Hg concentration in leaf litterfall, leaf litterfall Hg deposition and mean accumulated total atmospheric mercury (AccuTGM) concentration during foliage growing seasons from 2011 to 2019. (a) is for MEB forest and (b) for SMD forest.

That leads us to examine the influence of tree physiological processes that control foliage uptake of atmospheric Hg⁰ and its subsequent accumulation and translocation. The important physiological parameters include but are not limited to the inconsistent tree growth, rate of photosynthesis, stomata conductance, transpiration rate, foliage lifespan and canopy characteristics (Arnold et al., 2018; Erickson et al., 2003; Laacouri et al., 2013; Luo et al., 2016; Stamenkovic & Gustin, 2009; Wang, Yuan, et al., 2020; Wright & Zhang, 2015), all of which are sensitive to environmental and climatic conditions. The litterfall Hg concentration shows a significant anticorrelation to the average precipitation during the foliage lifespan in 2011–2014 and 2015–2016 (Figure 3b; $r = -0.62$, $P < 0.01$ for MEB in 2011–2014, and $r = -0.66$, $P < 0.01$ for MEB and SMD in 2015–2016 by t -test), but insignificant correlations in 2017–2019 non-drought periods (Figure S2 in Supporting Information S1). We postulated that drought events affect Hg concentration in litterfall because of the water stress that influences tree physiological processes. Moreover, another potential cause is that the lower precipitation washing through the canopy leads to more deposited Hg possibly absorbed by foliage. We recommend further studies to verify this issue.

Water stress can affect Hg accumulation in litterfall in multiple ways. First, it affects tree growth by influencing the rate of net photosynthesis, stomata conductance, and transpiration rate (Seyoum et al., 2012). The decrease of stomata conductance and transpiration rate reduces atmospheric Hg⁰ uptake and subsequently decrease Hg

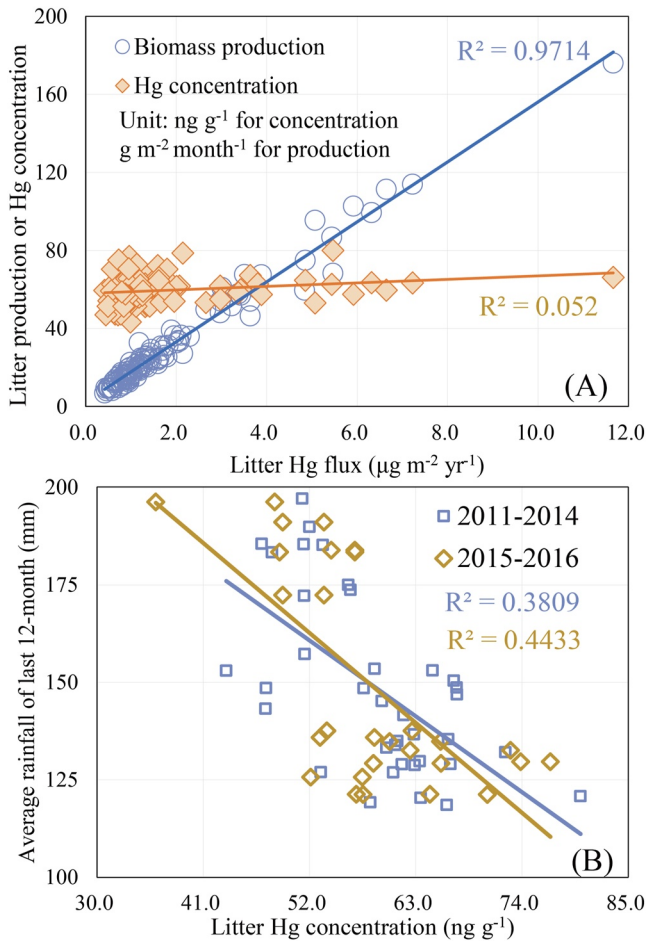


Figure 3. (a) Monthly litterfall mercury flux versus litterfall production or mercury concentration from 2011 to 2019 in MEB and SMD forests; (b) litterfall Hg concentration versus average precipitation during foliage lifespan (last 12-month before litterfall sampled) during 2011–2014 and 2015–2016.

accumulation in foliage (negative effect). It could also reduce Hg re-emission and increase Hg accumulation in foliage (positive effect) (Teixeira et al., 2018). Water stress also provokes leaf senescence, shortens foliage lifespan, reduces its exposure to atmospheric Hg^0 (negative effect), and promotes nutrient translocation before the leaf abscission, which significantly decreases the mass density (Ishida et al., 2006). During leaf abscission, Hg in foliage is immobilized due to sorption by macromolecular organic matters and/or the formation of nanoparticles (Cui et al., 2014; Manceau et al., 2018). The decreasing mass density and the immobility of Hg increase Hg concentration after leaf senescence (positive effect). Several studies on evergreen broadleaf tree species have reported 20%–50% greater Hg concentration in litters than in mature foliage (Buch et al., 2015; Teixeira et al., 2012, 2018). The positive effects from the water stress are higher than the negative effects at ASSFERS because of the elevated litterfall Hg concentration during drought periods. Finally, the continuous drought events can significantly affect water use efficiency, making the impacts over a long period of time after the drought (i.e., resulting in a distinct response lag; Section S1 in Supporting Information S1) (Linger et al., 2020; Thibault & Brown, 2008).

We attribute the increasing Hg concentration in litterfall of MEB forest during 2011–2014 to the effects from continued drought events, and the decreasing trend of Hg concentration in 2015–2016 to the restoration of rainfall ($\text{RDI} > 0$, Figure 1a) that relieved the water stress. Due to the elevated litterfall biomass production and litterfall Hg concentration caused by droughts in MEB forest in 2011–2014, we observed an increasing trend of litterfall Hg deposition (Figure 2a). Though without litterfall Hg data during 2014–2015, we speculate that the litterfall Hg concentrations remain at the high level because of the response lag between water stress and annual rhythms of tress species.

3.3. Impacts From Extreme Weather on Soil Hg Content

During 2007–2020, the Hg concentration in the MEB forest varies from 135 to 247 ng g^{-1} ($197 \pm 18 \text{ ng g}^{-1}$, median = 195 ng g^{-1} , $n = 124$) in humus soil, and from 159 to 251 ng g^{-1} ($201 \pm 18 \text{ ng g}^{-1}$, median = 203 ng g^{-1} , $n = 124$) in the top 0–20 cm mineral soil. These values are comparable to earlier reported concentrations (Z. Y. Lu et al., 2016; Wang, Lin, Lu, et al., 2016).

The Hg concentration in humus soil of SMD forest is 70% lower ($116 \pm 48 \text{ ng g}^{-1}$, median = 108 ng g^{-1} , $n = 131$) than that in the MEB forest, and in top 0–20 cm mineral soil is half the concentration in the MEB forest (mean = $74 \pm 28 \text{ ng g}^{-1}$, median = 66 ng g^{-1} , $n = 149$). This is because of the lower litterfall Hg deposition and higher Hg loss via runoff at the top of the mountains in SMD forest (Z. Y. Lu et al., 2016). Different from MEB forest, the Hg concentration in humus soil of SMD is 60% higher than in the top 0–20 cm mineral soil.

Figures 4a and 4b show that Hg concentrations in MEB and SMD forests remain relatively consistent over the measurement period. A distinct increase of the humus soil Hg in MEB and SMD forests is absent during the sustained drought in 2011–2014 (all $P > 0.05$ by ANOVA-test), though the litterfall Hg deposition increased, possibly due to the dilution of the Hg pool size (up to several mg m^{-2} Hg mass) (Wang, Lin, Lu et al., 2016; W. Yuan et al., 2020) in humus soils when compared to tens of $\mu\text{g m}^{-2} \text{yr}^{-1}$ litterfall Hg depositions. The snowstorm does not seem to significantly affect Hg concentration in humus soils of MEB forest compared to the data of 2014–2015 ($P = 0.73$ by independent t -test, Figure 4a), while there is an 18% decrease in 0–20 cm mineral soils. For SMD forest, the Hg concentration in humus soils increase one-time after the snow damage in 2015, and in 0–20 cm top mineral soils increase 50%.

The elevated Hg concentration caused by the snow damage is derived from the soil of canopy epiphyte cover. The subtropical evergreen broadleaf forest canopy has the intensive epiphyte cover which is composed of vegetation (such as moss, lichen, and ferns), dead roots, and humus soils formed by the senescence of vegetation

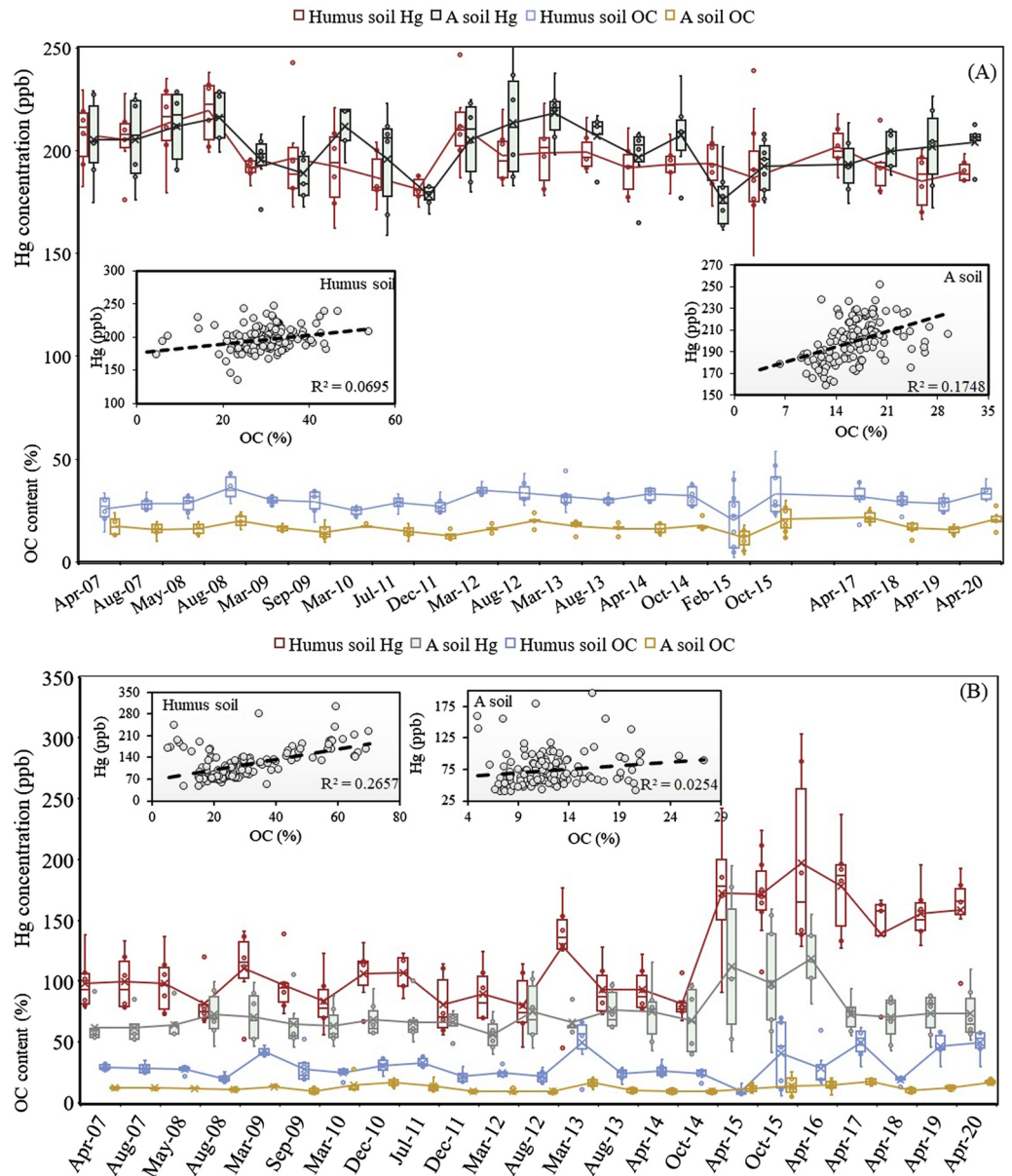


Figure 4. Variations of mercury concentration and organic carbon content (OC) in humus soil and 0–20 cm top mineral soil from 2007 to 2020. (a) at the MEB forest site, and (b) at the SMD forest site.

(Huang et al., 2019; L. Song et al., 2011). The enhanced Hg accumulation of moss and lichen (Olson et al., 2019; Wang, Yuan, Feng et al., 2019) results in up to $201 \pm 98 \text{ ng g}^{-1}$ Hg in soil under canopy epiphyte cover ($n = 62$, Table S2 in Supporting Information S1), nearly doubling the Hg concentration in humus soils of SMD forest ($116 \pm 48 \text{ ng g}^{-1}$). The snowstorm leads to large areas of canopy removal and substantial canopy epiphyte cover mixed into the forest floor, thus significant increasing soil Hg concentration in SMD forest ($p < 0.001$, by Independent Samples *t*-test). The insignificant fluctuation in humus Hg concentration of MEB forest after snow damage can be attributed to the similar Hg concentration in canopy epiphyte cover and humus soils ($201 \pm 98 \text{ ng g}^{-1}$ vs. $197 \pm 18 \text{ ng g}^{-1}$, $p = 0.28$, by Independent Samples *t*-test), as well as the thinner canopy epiphyte cover (Huang et al., 2019).

The gradual decrease of soil Hg concentration in SMD forest and in 0–20 cm top mineral soils of MEB forest after the snowstorm (during 2016–2018, Figure 4b) can be explained by two factors. One is the dilution by the translocation of downward low Hg from the deep soils (Demers et al., 2007; Wang, Lin, Lu, et al., 2016). The other is Hg

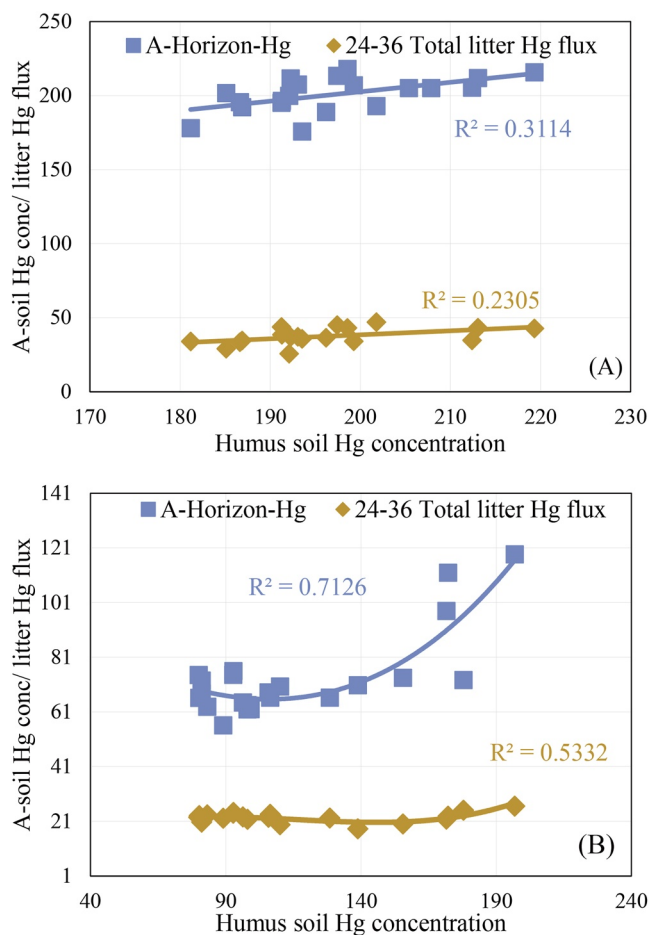


Figure 5. Hg concentration in humus soil (ng g^{-1}) versus in 0–20 cm top mineral soil (ng g^{-1}) and litterfall Hg deposition ($\mu\text{g g}^{-1} \text{yr}^{-1}$) over a 24–36 months period before soil sampling. (a) at the MEB forest site, and (b) at the SMD forest site. Linear regression (a) and third-order polynomial regression (b) were applied to fit the data. The litterfall Hg concentration of MEB was applied to represent the missing value of SMD in the estimation of litter Hg flux. This could induce uncertainties for the temporal trend.

washout with precipitation and runoff after the snow storm. Earlier findings suggest that snowmelt leads to a pulse of Hg-DOC (dissolved organic carbon) complex output in boreal forests (Douglas et al., 2017; Navratil et al., 2011). The Hg-containing runoff can be supported by the observed pulse of organic matter decrease after the snowstorm (Figures 4a and 4b), and the limited canopy epiphyte cover mixed into 0–20 cm mineral soils with elevated Hg concentration after the snow damage in the SMD forest (Figure 4b).

3.4. Soil Hg Variations Versus Litter Hg Inputs

Based on the isotopic evidence in our earlier study (Z. Lu et al., 2021; Wang, Yuan, Lu, et al., 2019; W. Yuan et al., 2020), >90% Hg in humus soil at ASSFERS is derived from the atmospheric Hg^0 deposition. Litterfall Hg deposition is the primary pathway of atmospheric Hg^0 deposition in forest ecosystems (Bishop et al., 2020; Wang, Bao, et al., 2016; Wang, Yuan, et al., 2020), and the variation of litterfall deposition can explain Hg concentration changes. However, the Hg concentrations in humus soils of MEB and SMD forests show insignificant correlation to current year litterfall Hg deposition. This is caused by the time lag between Hg release from litterfall to the soil. Our earlier studies suggest that, after 2-year decomposition, the Hg concentration in decomposing litter reach a level at 190 ng g^{-1} , comparable to the Hg concentration in humus soils (Wang, Lin, Lu, et al., 2016; W. Yuan et al., 2020). Figures 5a and 5b show the humus Hg concentration increases with increasing total litterfall Hg deposition that occurred 24–36 months earlier, consistent with the results of decomposition experiments. The 3–5 cm depth humus soil layer is formed in a 20-year period at ASSFERS (W. Yuan et al., 2020), which indicates that Hg in humus soil is derived from impacts of multiple-year litterfall Hg inputs and decomposition processes. The 24- to 36-month earlier litterfall Hg deposition only explains 23% variability of Hg concentration in the humus soil of MEB forest (Figure 5a), and shows a nonlinear relationship with humus soil Hg in SMD forest (Figure 5b). The humus soil Hg levels show a weak correlation to organic matter in the MEB forest, but a significant correlation in the SMD forest (Figures 4a and 4b). The correlation at the SMD site reflects Hg complexation with organic matters (Demers et al., 2013; Skjellberg et al., 2006). The weak correlation at the MEB site can be explained by the more complicated reactions among new Hg inputs, previous Hg accumulation, and carbon quick loss during the undergoing litter decomposition in this layer than in the SMD forest (Obriest et al., 2011; Wang, Lin, Lu, et al., 2016).

Given the timescale (in hundreds of years) needed for the formation of mineral soils (W. Yuan et al., 2020), the Hg concentration in the 0–20 cm mineral soil of MEB forest represents the result of combined effects from decomposition (Wang, Lin, Lu, et al., 2016; Wang, Yuan, Lu, et al., 2019), Hg^0 re-emission via the organic matter induced, microbial reductions (Yuan, Wang, et al., 2019; W. Yuan et al., 2020), and Hg leaching in soil profiles and runoff with DOC (Ma et al., 2015; Wang, Yuan, Lu, et al., 2019). These effects can explain the correlations between organic matters and Hg concentrations (Figure 4a), and between humus soil Hg and 0–20 cm top mineral soil Hg (Figure 5a) in MEB forest. However, we did not observe a significant correlation between Hg and organic matter in 0–20 cm top mineral soils of SMD (Figure 4b), possibly because of the mixing of 0–20 cm top mineral soils with disintegrated rock materials that contain low Hg and organic matter (Zhou et al., 2013). This is supported by the evidence that 38% lower organic matter in 0–20 cm top mineral soils of SMD forest than the values in 0–20 cm top mineral soils at the MEB site. The correlation between Hg in humus soil and in 0–20 cm top mineral soil is caused by the snowstorm induced humus layer Hg leaching into mineral soils (Figures 4b and 5b).

4. Conclusion

In this study, we found that droughts and snowstorms lead to a potential fluctuation of Hg storage in subtropical forest ecosystems. The snowstorm would immediately increase the Hg burden since substantial canopy Hg mixed into the forest floor, thus possibly increasing the soil Hg runoff and downstream Hg loading. In addition, a nearly 50% decrease in atmospheric Hg⁰ was found in 2011–2014, in contrast to the increase in litterfall Hg concentration and deposition caused by the sustained droughts. This is different from the observation at the Adirondack Mountains of New York State that 67% litterfall Hg flux decrease during 2004–2014 was attributed to the decrease of atmospheric Hg⁰ concentrations (Gerson et al., 2017). St Louis et al. (2019) also reported atmospheric Hg⁰ concentration decreased from 1.6 ng m⁻³ in 2005 to 1.2 ng m⁻³ in 2009, but Hg deposition in litterfall remained relatively constant at the remote experimental lake area, Northwestern Ontario. The different observations reflect the complex response of litterfall Hg to the atmospheric Hg⁰ decrease in forest ecosystems globally because of different climate impacts on Hg biogeochemical cycling (Jiskra et al., 2018; Obrist et al., 2018; Wang, Lin, Lu et al., 2016; Wang, Luo, et al., 2017; Wang, Yuan, Lin, et al., 2019).

The accelerated climate change could distinctly increase the unpredictability in assessing the effectiveness of Minamata Convention. Although extensive works have been carried out in quantifying Hg transport, accumulation and transformation in forest watershed (Grigal, 2003; Wang, Yuan & Feng, 2017; Wright et al., 2016), the large knowledge gaps limit our understanding on Hg biogeochemical processes and mass flow in response to climate change at the global scale. We recommend more observation and modeling studies on the ecological risk resulted from the climate events induced by the forced Hg input to terrestrial biomes.

Conflict of Interest

The authors declare no conflicts of interest relevant to this study.

Data Availability Statement

The temporal data sets of soil and litterfall Hg of 2019 and canopy moss cover Hg concentrations in Tables S1 and S2 in Supporting Information S1. The data sets are available at: https://figshare.com/articles/dataset/Yuan_et_al_data_Figshare_xlsx/17211899.

References

- Allan, C. J., Heyes, A., Roulet, N. T., St Louis, V. L., & Rudd, J. W. M. (2001). Spatial and temporal dynamics of mercury in Precambrian shield upland runoff. *Biogeochemistry*, 52(1), 13–40. <https://doi.org/10.1023/a:1026543418120>
- Arnold, J., Gustin, M. S., & Weisberg, P. J. (2018). Evidence for nonstomatal uptake of Hg by Aspen and translocation of Hg from foliage to tree rings in Austrian Pine. *Environmental Science & Technology*, 52(3), 1174–1182. <https://doi.org/10.1021/acs.est.7b04468>
- Bishop, K., Shanley, J. B., Riscassi, A., de Wit, H. A., Eklöf, K., Meng, B., et al. (2020). Recent advances in understanding and measurement of mercury in the environment: Terrestrial Hg cycling. *Science of the Total Environment*, 721, 137647. <https://doi.org/10.1016/j.scitotenv.2020.137647>
- Braune, B. M., Gaston, A. J., & Mallory, M. L. (2016). Temporal trends of mercury in eggs of five sympatrically breeding seabird species in the Canadian Arctic. *Environmental Pollution*, 214, 124–131. <https://doi.org/10.1016/j.envpol.2016.04.006>
- Buch, A. C., Fernandes Correia, M. E., Teixeira, D. C., & Silva-Filho, E. V. (2015). Characterization of soil fauna under the influence of mercury atmospheric deposition in Atlantic Forest, Rio de Janeiro, Brazil. *Journal of Environmental Sciences*, 32, 217–227. <https://doi.org/10.1016/j.jes.2015.01.009>
- Burgess, N. M., Bond, A. L., Hebert, C. E., Neugebauer, E., & Champoux, L. (2013). Mercury trends in herring gull (*Larus argentatus*) eggs from Atlantic Canada, 1972–2008: Temporal change or dietary shift? *Environmental Pollution*, 172, 216–222. <https://doi.org/10.1016/j.envpol.2012.09.001>
- Bushey, J. T., Driscoll, C. T., Mitchell, M. J., Selvendiran, P., & Montesdeoca, M. R. (2008). Mercury transport in response to storm events from a northern forest landscape. *Hydrological Processes*, 22(25), 4813–4826. <https://doi.org/10.1002/hyp.7091>
- Cheng, Q., Gao, L., Zhong, F., Zuo, X., & Ma, M. (2020). Spatiotemporal variations of drought in the Yunnan-Guizhou Plateau, southwest China, during 1960–2013 and their association with large-scale circulations and historical records. *Ecological Indicators*, 112, 106041. <https://doi.org/10.1016/j.ecolind.2019.106041>
- Cui, L. W., Feng, X. B., Lin, C. J., Wang, X. M., Meng, B., Wang, X., & Wang, H. (2014). Accumulation and Translocation of ¹⁹⁸Hg in four crop species. *Environmental Toxicology & Chemistry*, 33(2), 334–340. <https://doi.org/10.1002/etc.2443>
- D'Amore, F., Bencardino, M., Cinnirella, S., Sprovieri, F., & Pirrone, N. (2015). Data quality through a web-based QA/QC system: Implementation for atmospheric mercury data from the global mercury observation system. *Environmental Science—Processes & Impacts*, 17(8), 1482–1491. <https://doi.org/10.1039/c5em00205b>
- Demers, J. D., Driscoll, C. T., Fahey, T. J., & Yavitt, J. B. (2007). Mercury cycling in litter and soil in different forest types in the Adirondack region. *Ecological Applications*, 17(5), 1341–1351. <https://doi.org/10.1890/06-1697.1>

Acknowledgments

This work was funded by National Natural Science Foundation of China (41829701, 41977272, and 41921004) and K.C. Wong Education Foundation.

- Demers, J. D., Yavitt, J. B., Driscoll, C. T., & Montesdeoca, M. R. (2013). Legacy mercury and stoichiometry with C, N, and S in soil, pore water, and stream water across the upland-wetland interface: The influence of hydrogeologic setting. *Journal of Geophysical Research: Biogeosciences*, *118*(2), 825–841. <https://doi.org/10.1002/jgrg.20066>
- Douglas, T. A., Loseto, L. L., Macdonald, R. W., Outridge, P., Dommergue, A., Poulain, A., et al. (2012). The fate of mercury in Arctic terrestrial and aquatic ecosystems, a review. *Environmental Chemistry*, *9*(4), 321–355. <https://doi.org/10.1071/en11140>
- Douglas, T. A., Sturm, M., Blum, J. D., Polashensld, C., Stuefer, S., Hiemstra, C., et al. (2017). A pulse of mercury and major ions in snowmelt runoff from a small Arctic Alaska watershed. *Environmental Science & Technology*, *51*(19), 11145–11155. <https://doi.org/10.1021/acs.est.7b03683>
- Eklöf, K., Meili, M., Akerblom, S., von Bromssen, C., & Bishop, K. (2013). Impact of stump harvest on run-off concentrations of total mercury and methylmercury. *Forest Ecology and Management*, *290*, 83–94. <https://doi.org/10.1016/j.foreco.2012.05.039>
- Eriksen, J. A., Gustin, M. S., Schorran, D. E., Johnson, D. W., Lindberg, S. E., & Coleman, J. S. (2003). Accumulation of atmospheric mercury in forest foliage. *Atmospheric Environment*, *37*(12), 1613–1622. [https://doi.org/10.1016/s1352-2310\(03\)00008-6](https://doi.org/10.1016/s1352-2310(03)00008-6)
- Evans, M., Muir, D., Brua, R. B., Keating, J., & Wang, X. (2013). Mercury trends in predatory fish in Great Slave Lake: The influence of temperature and other climate drivers. *Environmental Science & Technology*, *47*(22), 12793–12801. <https://doi.org/10.1021/es402645x>
- Evers, D. C., Han, Y. J., Driscoll, C. T., Kamman, N. C., Goodale, M. W., Lambert, K. F., et al. (2007). Biological mercury hotspots in the North-eastern United States and Southeastern Canada. *BioScience*, *57*(1), 29–43. <https://doi.org/10.1641/b570107>
- Feng, X. B., Foucher, D., Hintelmann, H., Yan, H. Y., He, T. R., & Qiu, G. L. (2010). Tracing mercury contamination sources in sediments using mercury isotope compositions. *Environmental Science & Technology*, *44*(9), 3363–3368. <https://doi.org/10.1021/es9039488>
- Gabriel, M. C., Williamson, D. G., Brooks, S., Zhang, H., & Lindberg, S. (2005). Spatial variability of mercury emissions from soils in a south-eastern US urban environment. *Environmental Geology*, *48*(7), 955–964. <https://doi.org/10.1007/s00254-005-0043-x>
- Gastineau, G., & Soden, B. J. (2009). Model projected changes of extreme wind events in response to global warming. *Geophysical Research Letters*, *36*, L10810. <https://doi.org/10.1029/2009gl037500>
- Gerson, J. R., Driscoll, C. T., Demers, J. D., Sauer, A. K., Blackwell, B. D., Montesdeoca, M. R., et al. (2017). Deposition of mercury in forests across a montane elevation gradient: Elevational and seasonal patterns in methylmercury inputs and production. *Journal of Geophysical Research: Biogeosciences*, *122*(8), 1922–1939. <https://doi.org/10.1002/2016jgrg003721>
- Grigal, D. F. (2003). Mercury sequestration in forests and peatlands: A review. *Journal of Environmental Quality*, *32*(2), 393–405. <https://doi.org/10.2134/jeq2003.3930>
- Hanson, P. J., Lindberg, S. E., Tabberer, T. A., Owens, J. G., & Kim, K. H. (1995). Foliar exchange of mercury-vapor—Evidence for a compensation point. *Water, Air, & Soil Pollution*, *80*(1–4), 373–382. https://doi.org/10.1007/978-94-011-0153-0_41
- Huang, J. B., Liu, W. Y., Li, S., Song, L., Lu, H. Z., Shi, X. M., et al. (2019). Ecological stoichiometry of the epiphyte community in a subtropical forest canopy. *Ecology and Evolution*, *9*(24), 14394–14406. <https://doi.org/10.1002/ece3.5875>
- Ishida, A., Diloksumpun, S., Ladpala, P., Staporn, D., Panuthai, S., Gamo, M., et al. (2006). Contrasting seasonal leaf habits of canopy trees between tropical dry-deciduous and evergreen forests in Thailand. *Tree Physiology*, *26*(5), 643–656. <https://doi.org/10.1093/treephys/26.5.643>
- Jiskra, M., Sonke, J. E., Obrist, D., Bieser, J., Ebinghaus, R., Myhre, C. L., et al. (2018). A vegetation control on seasonal variations in global atmospheric mercury concentrations. *Nature Geoscience*, *11*(4), 244–250. <https://doi.org/10.1038/s41561-018-0078-8>
- Laacouri, A., Nater, E. A., & Kolka, R. K. (2013). Distribution and uptake dynamics of mercury in leaves of common deciduous tree species in Minnesota, USA. *Environmental Science & Technology*, *47*(18), 10462–10470. <https://doi.org/10.1021/es401357z>
- Lee, Y. H., Bishop, K. H., & Munthe, J. (2000). Do concepts about catchment cycling of methylmercury and mercury in boreal catchments stand the test of time? Six years of atmospheric inputs and runoff export at Svartberget, northern Sweden. *Science of the Total Environment*, *260*(1–3), 11–20. [https://doi.org/10.1016/s0048-9697\(00\)00538-6](https://doi.org/10.1016/s0048-9697(00)00538-6)
- Linger, E., Hogan, J. A., Cao, M., Zhang, W.-F., Yang, X.-F., & Hu, Y.-H. (2020). Precipitation influences on the net primary productivity of a tropical seasonal rainforest in Southwest China: A 9-year case study. *Forest Ecology and Management*, *467*, 118153. <https://doi.org/10.1016/j.foreco.2020.118153>
- Liu, W., Fox, J. E. D., & Xu, Z. (2002). Biomass and nutrient accumulation in montane evergreen broad-leaved forest (*Lithocarpus xylocarpus* type) in Ailao Mountains, SW China. *Forest Ecology and Management*, *158*(1), 223–235. [https://doi.org/10.1016/S0378-1127\(00\)00716-7](https://doi.org/10.1016/S0378-1127(00)00716-7)
- Liu, W., Fox, J. E. D., & Xu, Z. (2003). Litterfall and nutrient dynamics in a montane moist evergreen broad-leaved forest in Ailao Mountains, SW China. *Plant Ecology*, *164*(2), 157–170. <https://doi.org/10.1023/A:1021201012950>
- Lu, Z., Yuan, W., Luo, K., & Wang, X. (2021). Litterfall mercury reduction on a subtropical evergreen broadleaf forest floor revealed by multi-element isotopes. *Environmental Pollution*, *268*, 115867. <https://doi.org/10.1016/j.envpol.2020.115867>
- Lu, Z. Y., Wang, X., Zhang, Y. P., Zhang, Y. J., Luo, K., & Sha, L. Q. (2016). High mercury accumulation in two subtropical evergreen forests in South China and potential determinants. *Journal of Environmental Management*, *183*, 488–496. <https://doi.org/10.1016/j.jenvman.2016.08.073>
- Luo, Y., Duan, L., Driscoll, C. T., Xu, G. Y., Shao, M. S., Taylor, M., et al. (2016). Foliage/atmosphere exchange of mercury in a subtropical coniferous forest in south China. *Journal of Geophysical Research: Biogeosciences*, *121*(7), 2006–2016. <https://doi.org/10.1002/2016jgrg003388>
- Ma, M., Wang, D., Sun, T., Zhao, Z., & Du, H. (2015). Forest runoff increase mercury output from subtropical forest catchments: An example from an alpine reservoir in a national nature reserve (southwestern China). *Environmental Science & Pollution Research*, *22*(4), 2745–2756. <https://doi.org/10.1007/s11356-014-3549-5>
- Manceau, A., Wang, J. X., Rovezzi, M., Glatzel, P., & Feng, X. B. (2018). Biogenesis of mercury-sulfur nanoparticles in plant leaves from atmospheric gaseous mercury. *Environmental Science & Technology*, *52*(7), 3935–3948. <https://doi.org/10.1021/acs.est.7b05452>
- Navratil, T., Rohovec, J., Hojdova, M., & Vach, M. (2011). Spring snowmelt and mercury export from a forested catchment in the Czech Republic, Central Europe. *Bulletin of Environmental Contamination and Toxicology*, *86*(6), 670–675. <https://doi.org/10.1007/s00128-011-0267-2>
- Obrist, D., Johnson, D. W., Lindberg, S. E., Luo, Y., Hararuk, O., Bracho, R., et al. (2011). Mercury distribution across 14 US Forests. Part I: Spatial patterns of concentrations in biomass, litter, and soils. *Environmental Science & Technology*, *45*(9), 3974–3981. <https://doi.org/10.1021/es104384m>
- Obrist, D., Kirk, J. L., Zhang, L., Sunderland, E. M., Jiskra, M., & Selin, N. E. (2018). A review of global environmental mercury processes in response to human and natural perturbations: Changes of emissions, climate, and land use. *Ambio*, *47*(2), 116–140. <https://doi.org/10.1007/s13280-017-1004-9>
- Olson, C. L., Jiskra, M., Sonke, J. E., & Obrist, D. (2019). Mercury in tundra vegetation of Alaska: Spatial and temporal dynamics and stable isotope patterns. *Science of the Total Environment*, *660*, 1502–1512. <https://doi.org/10.1016/j.scitotenv.2019.01.058>
- Orlowsky, B., & Seneviratne, S. I. (2012). Global changes in extreme events: Regional and seasonal dimension. *Climatic Change*, *110*(3–4), 669–696. <https://doi.org/10.1007/s10584-011-0122-9>

- Outridge, P. M., Mason, R. P., Wang, F., Guerrero, S., & Heimbürger-Boavida, L. E. (2018). Updated global and oceanic mercury budgets for the United Nations global mercury assessment 2018. *Environmental Science & Technology*, 52(20), 11466–11477. <https://doi.org/10.1021/acs.est.8b01246>
- Selin, H., Keane, S. E., Wang, S. X., Selin, N. E., Davis, K., & Bally, D. (2018). Linking science and policy to support the implementation of the Minamata Convention on Mercury. *Ambio*, 47(2), 198–215. <https://doi.org/10.1007/s13280-017-1003-x>
- Seyoum, Y., Fetene, M., Strobl, S., & Beck, E. (2012). Foliage dynamics, leaf traits, and growth of coexisting evergreen and deciduous trees in a tropical montane forest in Ethiopia. *Trees—Structure and Function*, 26(5), 1495–1512. <https://doi.org/10.1007/s00468-012-0723-6>
- Skylberg, U., Bloom, P. R., Qian, J., Lin, C. M., & Bleam, W. F. (2006). Complexation of mercury(II) in soil organic matter: EXAFS evidence for linear two-coordination with reduced sulfur groups. *Environmental Science & Technology*, 40(13), 4174–4180. <https://doi.org/10.1021/es0600577>
- Song, L., Liu, W. -Y., Ma, W. -Z., & Tan, Z. -H. (2011). Bole epiphytic bryophytes on *Lithocarpus xylocarpus* (Kurz) Markgr in the Ailao Mountains, SW China. *Ecological Research*, 26(2), 351–363. <https://doi.org/10.1007/s1284-010-0790-3>
- Song, X., James Aaron, H., Brown, C., Cao, M., & Yang, J. (2017). Snow damage to the canopy facilitates alien weed invasion in a subtropical montane primary forest in southwestern China. *Forest Ecology and Management*, 391, 275–281. <https://doi.org/10.1016/j.foreco.2017.02.031>
- Sproveri, F., Pirrone, N., Bencardino, M., D'Amore, F., Carbone, F., Cinnirella, S., et al. (2016). Atmospheric mercury concentrations observed at ground-based monitoring sites globally distributed in the framework of the GMOS network. *Atmospheric Chemistry and Physics*, 16(18), 11915–11935. <https://doi.org/10.5194/acp-16-11915-2016>
- Stamenkovic, J., & Gustin, M. S. (2009). Nonstomatal versus stomatal uptake of atmospheric Mercury, *Environmental Science & Technology*, 43(5), 1367–1372, DOI <https://doi.org/10.1021/es801583a>
- St Louis, V. L., Graydon, J. A., Lehnher, I., Amos, H. M., Sunderland, E. M., St. Pierre, K. A., et al. (2019). Atmospheric concentrations and wet/dry loadings of mercury at the remote experimental lakes area, northwestern Ontario, Canada. *Environmental Science & Technology*, 53(14), 8017–8026. <https://doi.org/10.1021/acs.est.9b01338>
- Sun, S., Ma, M., He, X., Obrist, D., Zhang, Q., Yin, X., et al. (2020). Vegetation mediated mercury flux and atmospheric mercury in the alpine permafrost region of the Central Tibetan Plateau. *Environmental Science & Technology*, 54(10), 6043–6052. <https://doi.org/10.1021/acs.est.9b06636>
- Sun, X. J., Wang, K., Kang, S. C., Guo, J. M., Zhang, G. S., Huang, J., et al. (2017). The role of melting alpine glaciers in mercury export and transport: An intensive sampling campaign in the Qugaqie Basin, inland Tibetan Plateau. *Environmental Pollution*, 220, 936–945. <https://doi.org/10.1016/j.envpol.2016.10.079>
- Tang, Y., Wang, S., Wu, Q., Liu, K., Wang, L., Li, S., et al. (2018). Recent decrease trend of atmospheric mercury concentrations in East China: The influence of anthropogenic emissions. *Atmospheric Chemistry and Physics Discussions*, 1–30. <https://doi.org/10.5194/acp-2017-1203>
- Teixeira, D. C., Lacerda, L. D., & Silva-Filho, E. V. (2018). Foliar mercury content from tropical trees and its correlation with physiological parameters in situ. *Environmental Pollution*, 242, 1050–1057. <https://doi.org/10.1016/j.envpol.2018.07.120>
- Teixeira, D. C., Montezuma, R. C., Oliveira, R. R., & Silva, E. V. (2012). Litterfall mercury deposition in Atlantic forest ecosystem from SE–Brazil. *Environmental Pollution*, 164, 11–15. <https://doi.org/10.1016/j.envpol.2011.10.032>
- Thibault, K. M., & Brown, J. H. (2008). Impact of an extreme climatic event on community assembly. *Proceedings of the National Academy of Sciences of the United States of America*, 105(9), 3410–3415. <https://doi.org/10.1073/pnas.0712282105>
- Tsakiris, G., Pangalou, D., & Vangelis, H. (2007). Regional drought assessment based on the Reconnaissance Drought Index (RDI). *Water Resources Management*, 21(5), 821–833. <https://doi.org/10.1007/s11269-006-9105-4>
- UN-Environment (2019). *Global Mercury Assessment 2018, UN-Environment Programme*. Geneva, Switzerland: Chemicals and Health Branch.
- Walkley, A. (1947). A critical examination of a rapid method for determining organic carbon in soils—Effect of variations in digestion conditions and of inorganic soil constituents. *Soil Science*, 63(4). <https://doi.org/10.1097/00010694-194704000-00001>
- Wang, F., Outridge, P. M., Feng, X., Meng, B., Heimbürger-Boavida, L. E., & Mason, R. P. (2019). How closely do mercury trends in fish and other aquatic wildlife track those in the atmosphere?—Implications for evaluating the effectiveness of the Minamata Convention. *Science of the Total Environment*, 674, 58–70. <https://doi.org/10.1016/j.scitotenv.2019.04.101>
- Wang, X., Bao, Z., Lin, C.-J., Yuan, W., & Feng, X. (2016). Assessment of global mercury deposition through litterfall. *Environmental Science & Technology*, 50(16), 8548–8557. <https://doi.org/10.1021/acs.est.5b06351>
- Wang, X., Lin, C.-J., & Feng, X. (2014). Sensitivity analysis of an updated bidirectional air-surface exchange model for elemental mercury vapor. *Atmospheric Chemistry and Physics*, 14(12), 6273–6287. <https://doi.org/10.5194/acp-14-6273-2014>
- Wang, X., Lin, C.-J., Lu, Z., Zhang, H., Zhang, Y., & Feng, X. (2016). Enhanced accumulation and storage of mercury on subtropical evergreen forest floor: Implications on mercury budget in global forest ecosystems. *Journal of Geophysical Research: Biogeosciences*, 121(8), 2096–2109. <https://doi.org/10.1002/2016jg003446>
- Wang, X., Lin, C.-J., Yuan, W., Sommar, J., Zhu, W., & Feng, X. (2016). Emission-dominated gas exchange of elemental mercury vapor over natural surfaces in China. *Atmospheric Chemistry and Physics*, 16(17), 11125–11143. <https://doi.org/10.5194/acp-16-11125-2016>
- Wang, X., Luo, J., Yin, R., Yuan, W., Lin, C.-J., Sommar, J., et al. (2017). Using mercury isotopes to understand mercury accumulation in the Montane forest floor of the Eastern Tibetan Plateau. *Environmental Science & Technology*, 51(2), 801–809. <https://doi.org/10.1021/acs.est.6b03806>
- Wang, X., Luo, J., Yuan, W., Lin, C. J., Wang, F., Liu, C., et al. (2020). Global warming accelerates uptake of atmospheric mercury in regions experiencing glacier retreat. *Proceedings of the National Academy of Sciences of the United States of America*, 117(4), 2049–2055. <https://doi.org/10.1073/pnas.1906930117>
- Wang, X., Yuan, W., & Feng, X. (2017). Global review of mercury biogeochemical processes in forest ecosystems. *Progress in Chemistry*, 29(9), 970–980. <https://doi.org/10.7536/pc170343>
- Wang, X., Yuan, W., Feng, X., Wang, D., & Luo, J. (2019). Moss facilitating mercury, lead and cadmium enhanced accumulation in organic soils over glacial erratic at Mt. Gongga, China. *Environmental Pollution*, 254, 112974. <https://doi.org/10.1016/j.envpol.2019.112974>
- Wang, X., Yuan, W., Lin, C. J., Luo, J., Wang, F., Feng, X., et al. (2020). Underestimated sink of atmospheric mercury in a deglaciated forest chronosequence. *Environmental Science & Technology*, 54(13), 8083–8093. <https://doi.org/10.1021/acs.est.0c01667>
- Wang, X., Yuan, W., Lin, C. J., Zhang, L. M., Zhang, H., & Feng, X. B. (2019). Climate and vegetation as primary drivers for global mercury storage in surface soil. *Environmental Science & Technology*, 53(18), 10665–10675. <https://doi.org/10.1021/acs.est.9b02386>
- Wang, X., Yuan, W., Lu, Z. Y., Lin, C. J., Yin, R. S., Li, F., & Feng, X. B. (2019). Effects of precipitation on mercury accumulation on subtropical Montane Forest floor: Implications on Climate Forcing. *Journal of Geophysical Research: Biogeosciences*, 124(4), 959–972. <https://doi.org/10.1029/2018jg004809>

- Wang, X., Zhang, H., Lin, C.-J., Fu, X., Zhang, Y., & Feng, X. (2015). Transboundary transport and deposition of Hg emission from spring-time biomass burning in the Indo-China Peninsula. *Journal of Geophysical Research: Atmospheres*, *120*(18), 9758–9771. <https://doi.org/10.1002/2015JD023525>
- Wright, L. P., Zhang, L., & Marsik, F. J. (2016). Overview of mercury dry deposition, litterfall, and throughfall studies. *Atmospheric Chemistry and Physics*, *16*(21), 13399–13416. <https://doi.org/10.5194/acp-16-13399-2016>
- Wright, L. P., & Zhang, L. M. (2015). An approach estimating bidirectional air-surface exchange for gaseous elemental mercury at AMNet sites. *Journal of Advances in Modeling Earth Systems*, *7*(1), 35–49. <https://doi.org/10.1002/2014ms000367>
- Xu, Y., Zhang, Y., Yang, J., & Lu, Z. (2020). Influence of tree functional diversity and stand environment on fine root biomass and necromass in four types of evergreen broad-leaved forests. *Global Ecology and Conservation*, *21*, e00832. <https://doi.org/10.1016/j.gecco.2019.e00832>
- Yu, B., Fu, X., Yin, R., Zhang, H., Wang, X., Lin, C.-J., et al. (2016). Isotopic composition of atmospheric mercury in China: New evidence for sources and transformation processes in air and in vegetation. *Environmental Science & Technology*, *50*(17), 9262–9269. <https://doi.org/10.1021/acs.est.6b01782>
- Yuan, W., Sommar, J., Lin, C.-J., Wang, X., Li, K., Liu, Y., et al. (2019). Stable isotope evidence shows re-emission of elemental mercury vapor occurring after reductive loss from foliage. *Environmental Science & Technology*, *53*(2), 651–660. <https://doi.org/10.1021/acs.est.8b04865>
- Yuan, W., Wang, X., Lin, C.-J., Sommar, J., Lu, Z., & Feng, X. (2019). Process factors driving dynamic exchange of elemental mercury vapor over soil in broadleaf forest ecosystems. *Atmospheric Environment*, *219*, 117047. <https://doi.org/10.1016/j.atmosenv.2019.117047>
- Yuan, W., Wang, X., Lin, C. J., Wu, C., Zhang, L., Wang, B., et al. (2020). Stable mercury isotope transition during postdepositional decomposition of biomass in a forest ecosystem over five centuries. *Environmental Science & Technology*, *54*(14), 8739–8749. <https://doi.org/10.1021/acs.est.0c00950>
- Zhang, H., Fu, X. W., Lin, C. J., Shang, L. H., Zhang, Y. P., Feng, X. B., & Lin, C. (2016). Monsoon-facilitated characteristics and transport of atmospheric mercury at a high-altitude background site in southwestern China. *Atmospheric Chemistry and Physics*, *16*(20), 13131–13148. <https://doi.org/10.5194/acp-16-13131-2016>
- Zhang, Y., Soerensen, A. L., Schartup, A. T., & Sunderland, E. M. (2020). A global model for methylmercury formation and uptake at the base of marine food webs. *Global Biogeochemical Cycles*, *34*(2). <https://doi.org/10.1029/2019gb006348>
- Zhang, Y. X., Jacob, D. J., Horowitz, H. M., Chen, L., Amos, H. M., Krabbenhoft, D. P., et al. (2016). Observed decrease in atmospheric mercury explained by global decline in anthropogenic emissions. *Proceedings of the National Academy of Sciences of the United States of America*, *113*(3), 526–531. <https://doi.org/10.1073/pnas.1516312113>
- Zhou, J., Feng, X. B., Liu, H. Y., Zhang, H., Fu, X. W., Bao, Z. D., et al. (2013). Examination of total mercury inputs by precipitation and litterfall in a remote upland forest of Southwestern China. *Atmospheric Environment*, *81*, 364–372. <https://doi.org/10.1016/j.atmosenv.2013.09.010>